

## 2025 Series - Study #4

# CFturbo BLADERUNNER

## Gas Turbine Design for a Turbopump



**Figure 1:** Launcher E-2 engine according to [1]

Today, rockets are used to transport satellites and humans into space. These rockets use a cluster of liquid-propellant engines to generate thrust in the lower stage – in some heavy-duty designs with solid-fuel boosters – and in the upper stage often a single liquid-propellant engine of the same type with a thrust nozzle adapted to the vacuum. The enormous thrust generated by a liquid rocket engine is created by the combustion of high mass flows of fuel and oxidizer in the combustion chamber and the subsequent expansion of the combustion gases in the thrust nozzle. In modern liquid rocket engines, the pressure in the combustion chamber reaches up to 30 MPa, with temperatures rising to an extreme 3,000°C. Fuel and oxidizer are stored in liquid state in thin-walled, cylindrical tanks pressurized to approximately 0.5 MPa. The liquid oxygen is cryogenic at -193°C, but even fuels that are liquid at normal ambient temperature are cooled down for maximum density. The two liquids are fed and their pressure increased to a level above the combustion chamber pressure by means of turbopumps.

Typically, each liquid-propellant engine has its own turbopump with two centrifugal pumps for fuel and oxidizer arranged on a common shaft. The centrifugal pumps are driven by an axial gas turbine, which is also mounted on this shaft and is supplied with combustion gases.

A distinction must be made between the two concepts of a **gas-generator cycle (GG cycle or open cycle, figure 2)** and a **staged combustion cycle (preburner cycle or closed cycle, figure 3)**. Rocket engines with an open cycle burn a small portion of liquid fuel and oxidizer, exhausting gas to drive a turbine and then discharge it into the environment through a separate nozzle. This design is relatively simple and reliable and is used, for example, in the SpaceX Merlin engines and in the Vulcain 2.1 of the Ariane 6.

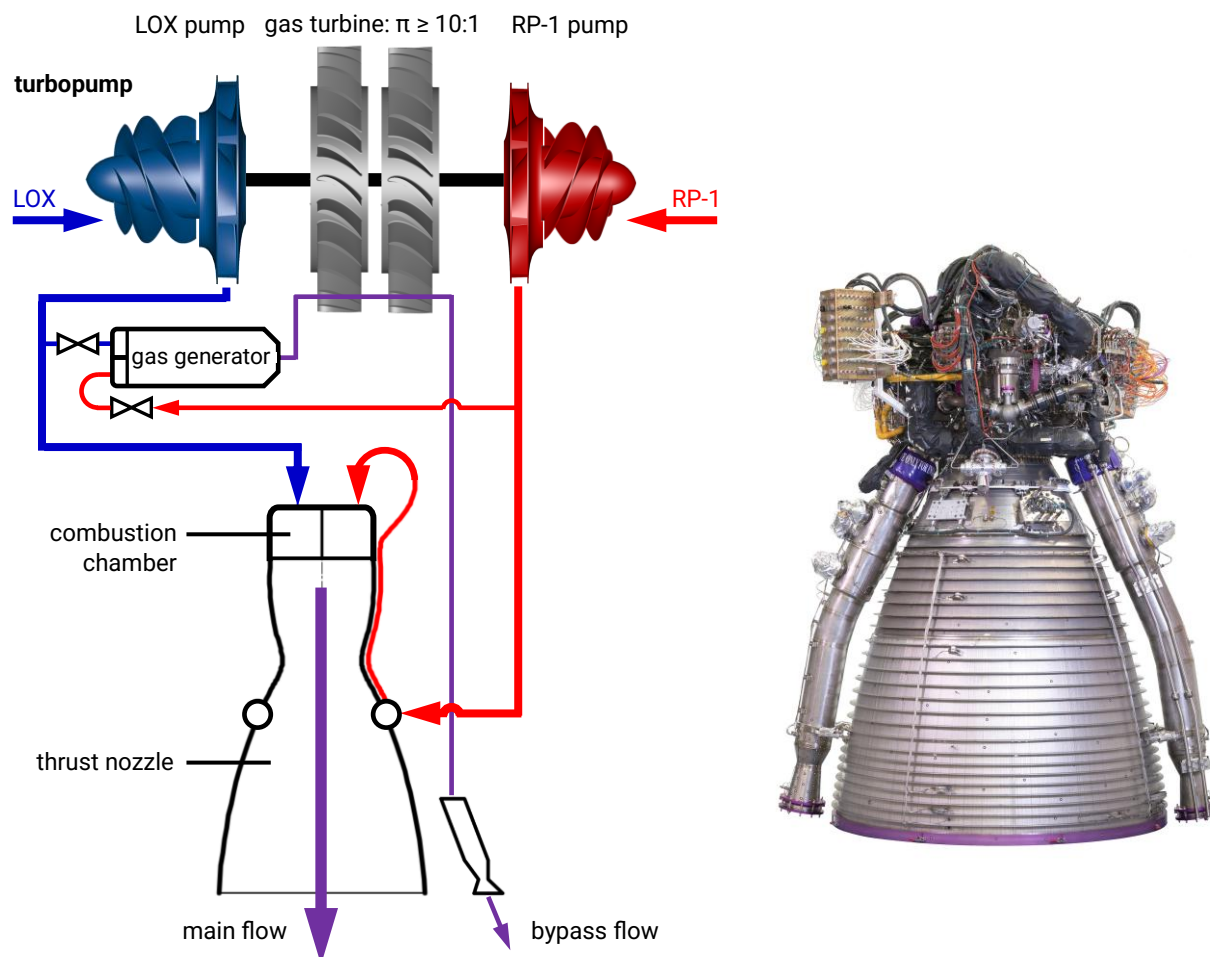


**Figure 2:** Simplified diagram of a gas-generator cycle engine with liquid oxygen (LOX) as oxidizer and RP-1 as fuel (left), Ariane 6 Vulcain 2.1 engine (right) according to [2]

The bypass flow that drives the gas turbine comprises only about 6% of the total mass flow. The drive power required for the turbopump is achieved here through high pressure ratios of  $\pi = 10:1$  or more. The gas turbine is designed as a two-stage constant pressure turbine. The main fuel flow cools the nozzle throat and the combustion chamber wall before being injected into the combustion chamber.

In the **staged combustion** concept, closed cycle engines supply the entire oxidizer mass flow and a small portion of the fuel mass flow in liquid form to a pre-combustion chamber in the case of oxidizer-rich pre-combustion. The combustion gas first drives the gas turbine, which is designed as a reaction turbine, and is then fed into the combustion chamber for further combustion with the main portion of the fuel. In fuel-rich pre-combustion, conversely, the entire fuel mass flow is fed into the pre-combustion chamber with a small portion of the oxidizer mass flow.

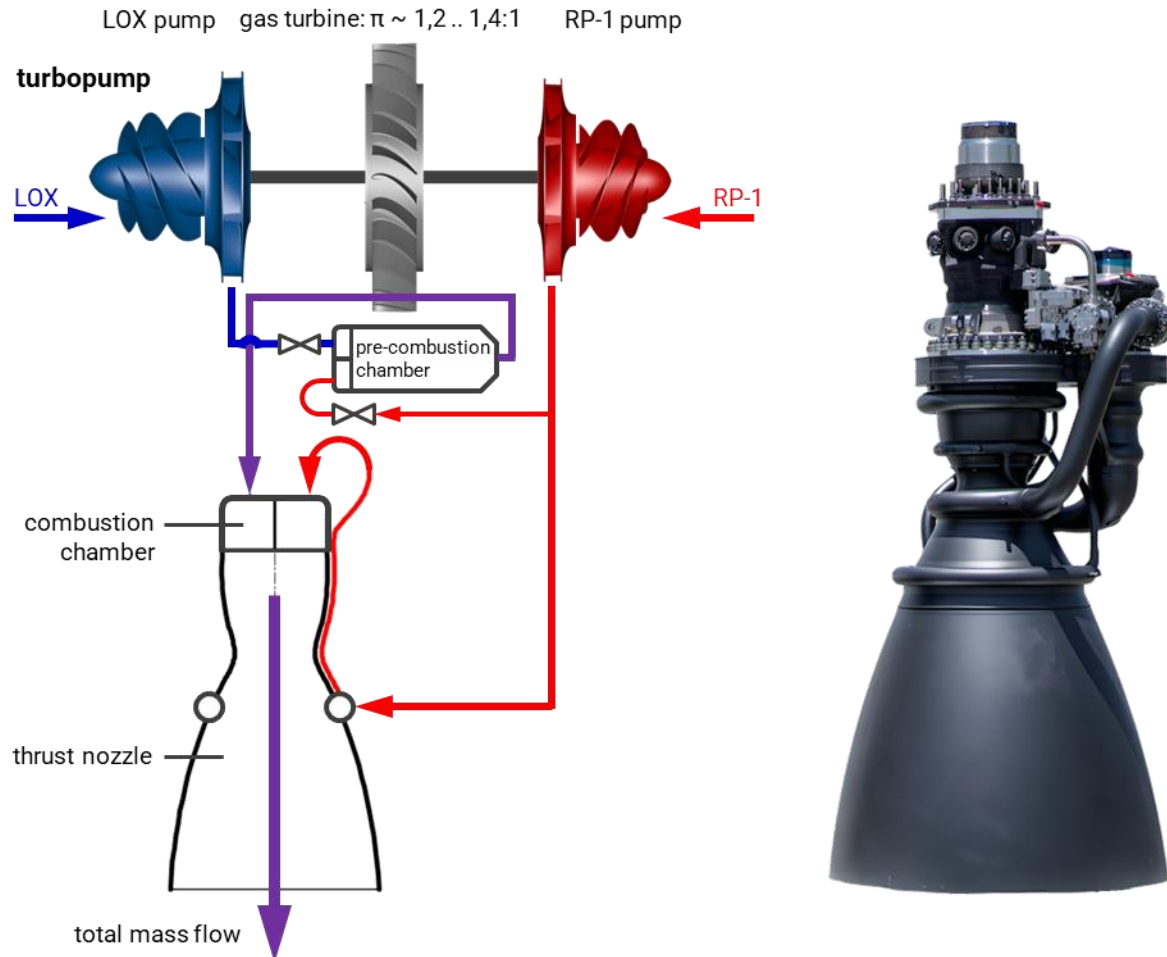
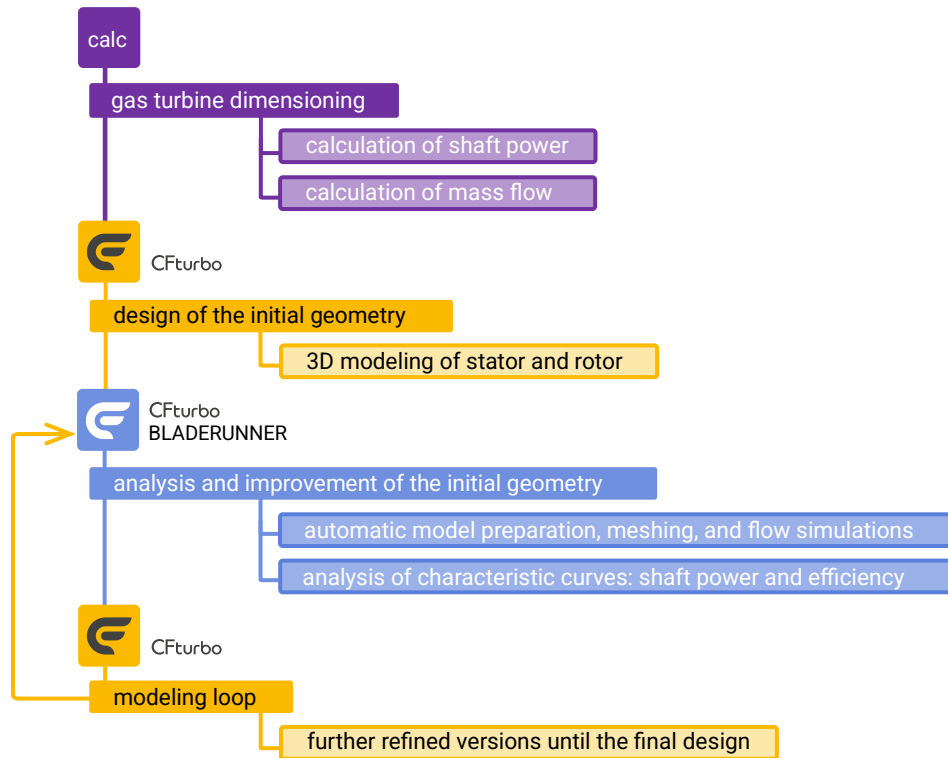


**Figure 3:** Simplified diagram of an engine with oxidizer-rich **staged combustion** (left), SpaceX Starship engine Raptor 3 (right) according to [3]

According to [4], **oxidizer-rich staged combustion (ORSC)** requires significantly lower pressures at the fuel pump outlet and in the pre-combustion chamber than fuel-rich staged combustion. Due to the corrosive effect of the combustion gas, this concept places high demands on the materials used in the gas turbine, valves, and pipes. Maturing to series production readiness in the 1980s, it is now used in almost all newly developed liquid engines due to its high energy efficiency, especially for use in upper stages, where every pound of fuel saved means one pound more payload.

The SpaceX Raptor engine, which runs on LOX/LCH<sub>4</sub> (liquid methane), even uses two separate turbopumps in **full-flow staged combustion** to adapt to the widely varying mass flows, one rich in oxidizer and one rich in fuel [5].

Study #3 in this series [6] dealt with the design of the LOX centrifugal pump with an inducer and a volute for a LOX/RP-1 rocket engine with  $F = 250$  kN thrust. Now, a suitable gas turbine for staged combustion is to be dimensioned and designed to drive the turbopump shown in Figure 3. The necessary steps for this are:



## Gas turbine dimensioning

### Determination of the required shaft power and the pre-combustion chamber mass flow

The specific impulse of the engine (a measure of its efficiency that compares the thrust generated to the total mass flow required) is assumed to be

$$I_{S,LOX/RP-1} = \frac{F}{\dot{m}_{total}} = 275 \cdot 9.81 \frac{Ns}{kg} = 2698 \frac{Ns}{kg} = 2698 \frac{m}{s} \stackrel{\text{def}}{=} 275 s$$

For maximum thrust, a rich mixture with an oxidizer-fuel ratio of

$$\frac{\dot{m}_{LOX}}{\dot{m}_{RP-1}} = 2.56$$

is produced in the combustion chamber.

The mass flows supplied by the centrifugal pumps then result in

$$\dot{m}_{total} = \dot{m}_{LOX} + \dot{m}_{RP-1} = \frac{F}{I_{S,LOX/RP-1}} = \frac{250 \text{ kN}}{2698 \text{ Ns/kg}} = 92.7 \frac{\text{kg}}{\text{s}}$$

$$\dot{m}_{LOX} = \frac{2,56}{2,56+1} \dot{m}_{ges} = 0.719 \cdot 92.7 \frac{\text{kg}}{\text{s}} = 66.6 \frac{\text{kg}}{\text{s}}$$

$$\dot{m}_{RP-1} = \dot{m}_{ges} - \dot{m}_{LOX} = 26.1 \frac{\text{kg}}{\text{s}}$$

With a total pressure increase of  $\Delta p_{t,CP} = 19.0 \text{ MPa}$  in the centrifugal pumps, a hydraulic efficiency of  $\eta_{hyd,CP} = 82.0\%$  with moderate cavitation in the inducer, and densities

$$\rho_{LOX, -193^\circ\text{C}} = 1141.9 \frac{\text{kg}}{\text{m}^3} \text{ according to [7] and } \rho_{RP-1, -7^\circ\text{C}} = 823.0 \frac{\text{kg}}{\text{m}^3} \text{ according to [8]}$$

the required shaft power with a 5% surcharge for bearing losses is

$$\begin{aligned} P_W &= 1.05 \cdot \frac{P_{hyd,CP}}{\eta_{hyd,CP}} = 1.05 \cdot \frac{\Delta p_{t,CP} (\dot{V}_{LOX} + \dot{V}_{RP-1})}{\eta_{hyd,CP}} = 1.05 \cdot \frac{\Delta p_{t,CP}}{\eta_{hyd,CP}} \left( \frac{\dot{m}_{LOX}}{\rho_{LOX, -193^\circ\text{C}}} + \frac{\dot{m}_{RP-1}}{\rho_{RP-1, -7^\circ\text{C}}} \right) \\ &= 1.05 \cdot \frac{19.0 \cdot 10^6 \frac{\text{N}}{\text{m}^2}}{0.82} \left( \frac{66.6 \frac{\text{m}^3}{\text{s}}}{1141.9} + \frac{26.1 \frac{\text{m}^3}{\text{s}}}{823.0} \right) = 2.2 \text{ MW} \end{aligned}$$

Combustion of a fraction of the RP-1 mass flow is sufficient to achieve this shaft power. The total temperature at which the exhaust gas enters the gas turbine should not exceed  $t_{t,GT} = 600^\circ\text{C}$ . The mass flow is heated by the reaction enthalpy of the fuel in the preburner (PB):

$$\dot{m}_{RP-1,PB} \cdot \Delta h_{RP-1} = c_{p,m} \cdot (\dot{m}_{LOX} \cdot \Delta T_{LOX,PB} + \dot{m}_{RP-1,PB} \cdot \Delta T_{RP-1,PB})$$

$$\Delta h_{RP-1} = 44,110 \frac{\text{kJ}}{\text{kg}} \quad \text{specific reaction enthalpy of RP-1 according to [7]}$$

$$c_{p,m} = 1.0 \frac{\text{kJ}}{\text{kg K}} \quad \text{mean specific heat capacity of the exhaust gas}$$

$$\Delta T_{LOX,PB} = 793 \text{ K} \quad \text{temperature increase from } t_{LOX} = -193^\circ\text{C} \text{ to } t_{t,GT} = 600^\circ\text{C}$$

$$\Delta T_{RP-1,PB} = 607 \text{ K} \quad \text{temperature increase from } t_{RP-1} = -7^\circ\text{C} \text{ to } t_{t,GT} = 600^\circ\text{C}$$

This gives the oxidizer-fuel ratio (O/F) of

$$O/F = \frac{\dot{m}_{LOX}}{\dot{m}_{RP-1,PB}} = \frac{\Delta h_{RP-1}}{c_{p,m} \cdot \Delta T_{LOX,PB}} - \frac{\Delta T_{RP-1,PB}}{\Delta T_{LOX,PB}} = \frac{44,110 \frac{\text{kJ}}{\text{kg}}}{1.0 \frac{\text{kJ}}{\text{kg K}} \cdot 793 \text{ K}} - \frac{607 \text{ K}}{793 \text{ K}} = 54.9 : 1$$

A more accurate calculation can be performed using the NASA CEA tool [9] or a CFD simulation of the combustion process. For the design of the gas turbine with CFturbo 2025, the material data for pure oxygen can be used for simplification at this high O/F ratio, neglecting components such as carbon monoxide or water vapor.

The RP-1 partial mass flow and the total mass flow through the pre-combustion chamber are calculated to a value of

$$\dot{m}_{RP-1,PB} = \frac{\dot{m}_{LOX}}{O/F} = \frac{66.6 \frac{kg}{s}}{54.9} = 1.2 \frac{kg}{s} ; \quad \dot{m}_{ges,PB} = \dot{m}_{LOX} + \dot{m}_{RP-1,PB} = 67.8 \frac{kg}{s}$$

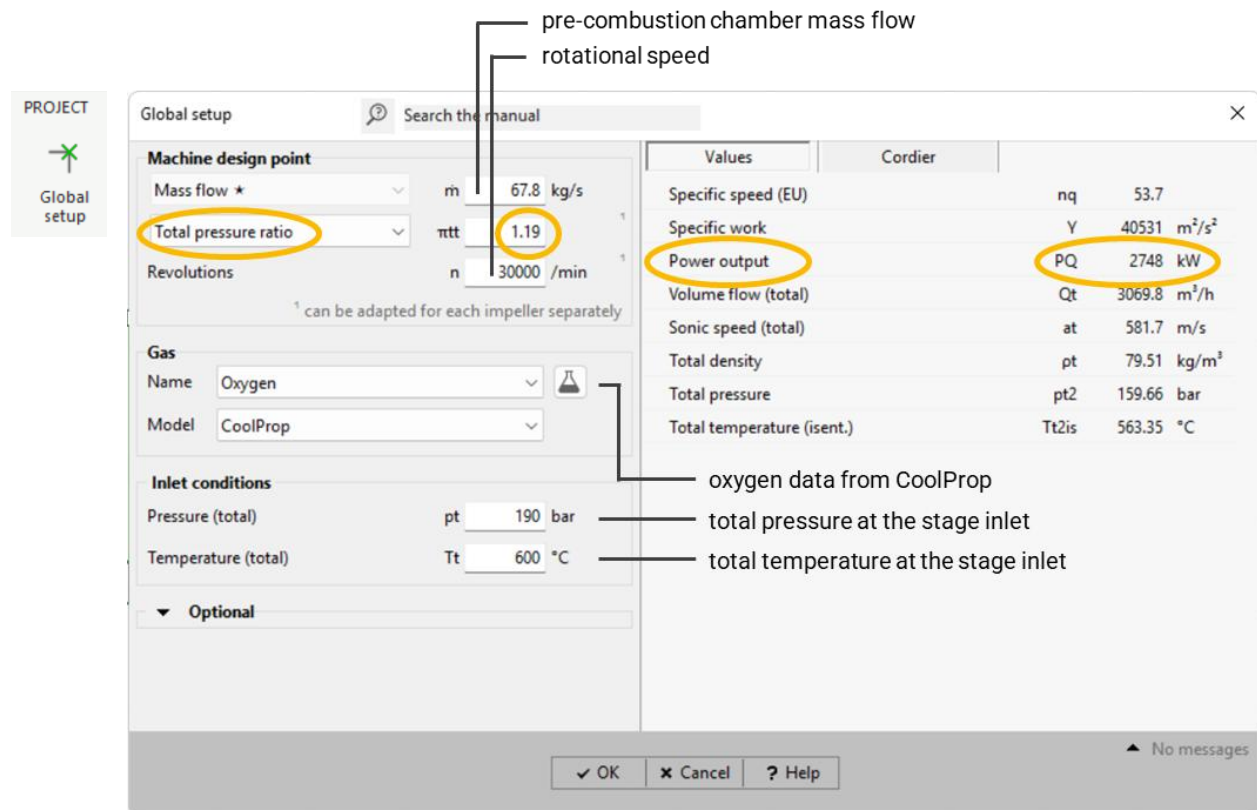
## Design of the initial geometry

### Step 1. Definition of the design point

CFturbo 2025 has its own module for designing gas turbine stages.

In the project setup, the calculated pre-combustion chamber mass flow and the speed of the turbo pump are first entered to define the design point. Oxygen from the CoolProp material database is selected as the fluid (figure 4). The gas state is determined by the total pressure built up by the centrifugal pumps and the selected total temperature of the exhaust gas.

For a total pressure ratio of  $\pi_{tt} = 1.19$ , CFturbo calculates a shaft power of 2.7 MW with isentropic expansion (orange circles). Assuming a gas turbine efficiency of 80%, the desired 2.2 MW is then achieved in the actual process.



pre-combustion chamber mass flow  
rotational speed

PROJECT  
Global setup

Global setup  ×

**Machine design point**

Mass flow \*

**Total pressure ratio**

Revolutions

<sup>1</sup> can be adapted for each impeller separately

**Gas**

Name

Model

**Inlet conditions**

Pressure (total)

Temperature (total)

▼ **Optional**

Values	Cordier
Specific speed (EU)	nq 53.7
Specific work	Y 40531 m <sup>2</sup> /s <sup>2</sup>
<b>Power output</b>	<b>PQ 2748 kW</b>
Volume flow (total)	Qt 3069.8 m <sup>3</sup> /h
Sonic speed (total)	at 581.7 m/s
Total density	pt 79.51 kg/m <sup>3</sup>
Total pressure	pt2 159.66 bar
Total temperature (isent.)	Tt2is 563.35 °C

oxygen data from CoolProp  
total pressure at the stage inlet  
total temperature at the stage inlet

OK  Cancel  Help

▲ No messages

**Figure 4:** Project setup for the gas turbine in CFturbo

## Design of the initial geometry

### Step 2. 3D modeling of stator and rotor

The gas turbine stage consists of a nozzle ring (stator) and a subsequent rotor. To achieve high efficiency of the stage, it is crucial that we:

- match the rotor speed and the stator flow redirection
- achieve a constant meridional velocity  $c_m$
- guide the flow on coaxial surfaces
- minimize outflow swirl

### Dimensioning of the annular duct diameter and of the blade height

For optimum power transmission in the rotor, the radial position of the annular duct and its height must be determined in such a way that the design of a flow-optimized rotor blade (and thus low-loss redirection of the fluid) is possible.

Geometries that fulfill this requirement have a specific ratio of blade speed  $u$  and power-dependent isentropic speed  $c_{0t}$ , as well as a specific relative blade height  $h/d_{s1}$ , and lie on or near the Cordier line (figure 5).

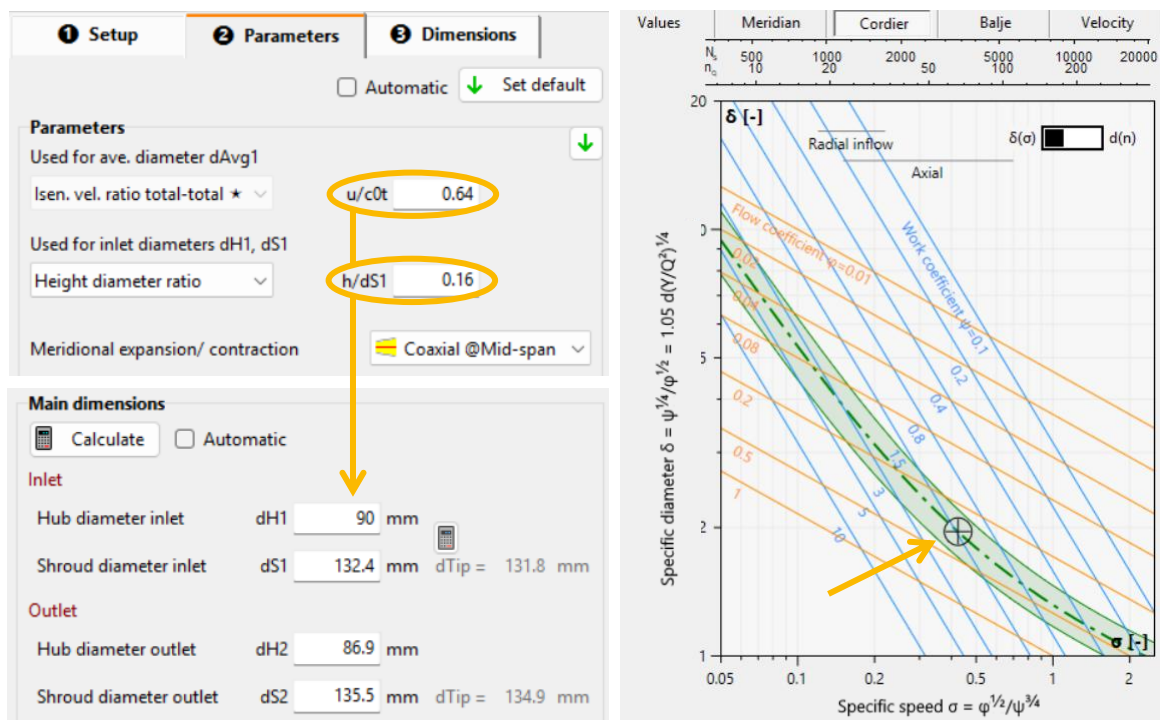


**Figure 5:** Dimensioning of the annular duct, position in the Cordier diagram

### Rotor design

CFturbo automatically generates three-dimensional blade geometries for the stator and rotor and compensates for the increase in flow rate during expansion in the rotor with a widening of the annular duct cross-section for constant meridional velocity  $c_m$ . Figure 6 shows the shrouded stator and the rotor with a tip clearance of 0.3 mm, with the Pipeln and PipeOut extensions for flow simulations.

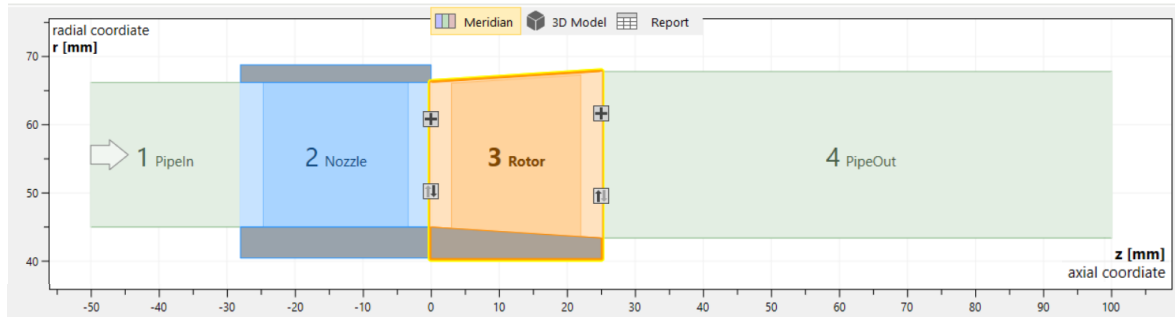


**Figure 6:** Annular duct of the gas turbine with stator and rotor in meridional section

When designing the rotor, CFturbo takes radial balance into account and twists the blade so that the pressure gradient across the blade height counteracts the centrifugal force in the fluid. The flow thus largely follows coaxial surfaces. A swirl-free outflow is achieved by the angle profile at the trailing edge (figure 7).

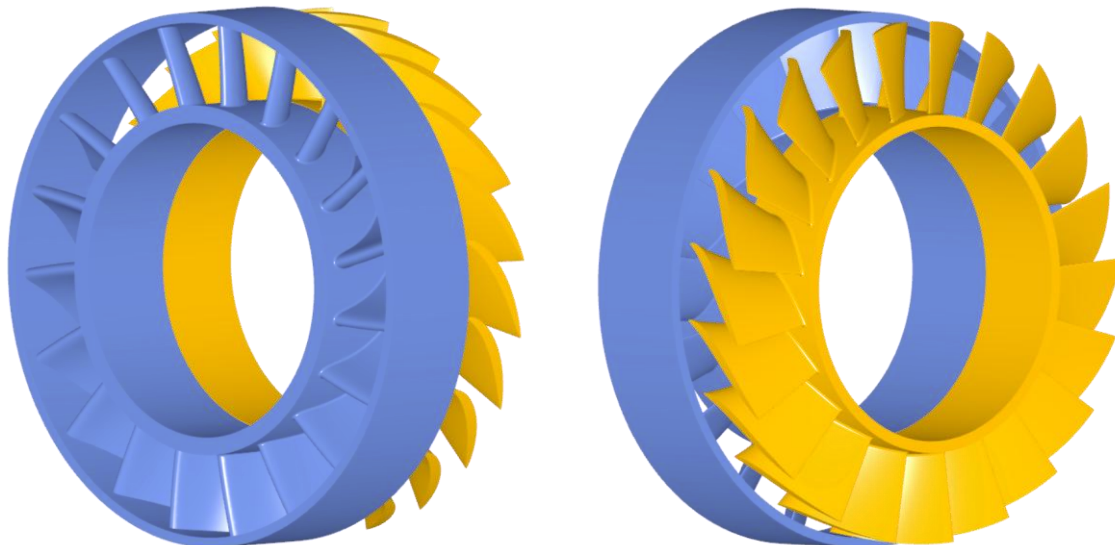


**Figure 7:** Initial geometry of stator (blue) and rotor (yellow) in CFturbo

### Analysis and improvement of the initial geometry

#### Systematic evaluation of variants with CFturbo BLADERUNNER

CFturbo BLADERUNNER takes the initial geometry for flow simulations directly from CFturbo, automatically meshes it, and applies the boundary conditions. Mesh refinements can be set individually for each surface element (figure 8).

To calculate the flow fields, CFturbo BLADERUNNER runs the Simerics MP solver, monitors the convergence progress, and displays the calculated characteristic curves in clear and concise diagrams (figure 9). For the initial geometry with the parameters  $u/c_{0t} = 0.64$  and  $h/d_{s1} = 0.16$ , an isentropic peak efficiency of 89.6% is already achieved, which can be increased to 91.6% by systematically changing these parameters until it drops again with an even larger annular duct ( $u/c_{0t} = 0.71$ ,  $h/d_{s1} = 0.16$ ).

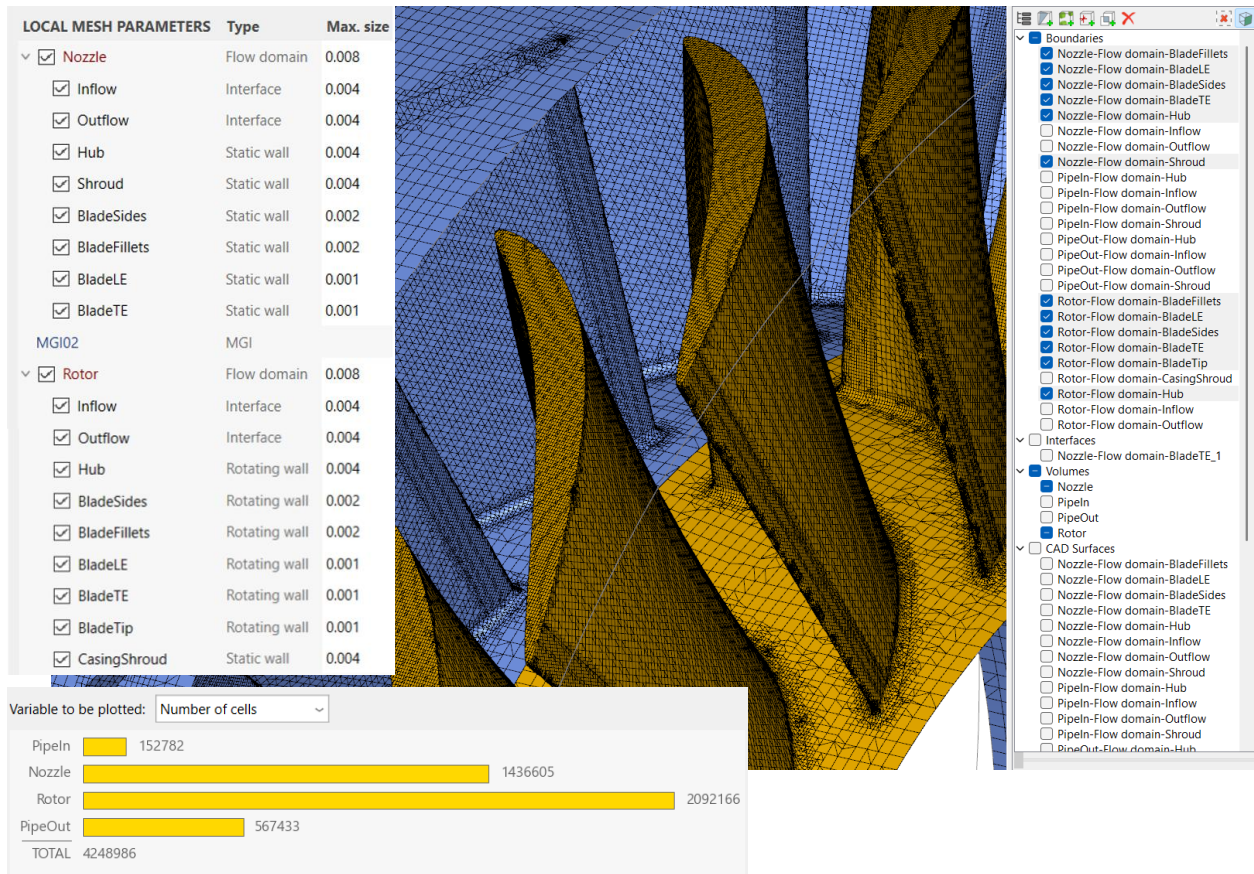


**Figure 8:** Mesh settings and cell distribution statistics in CFturbo BLADERUNNER

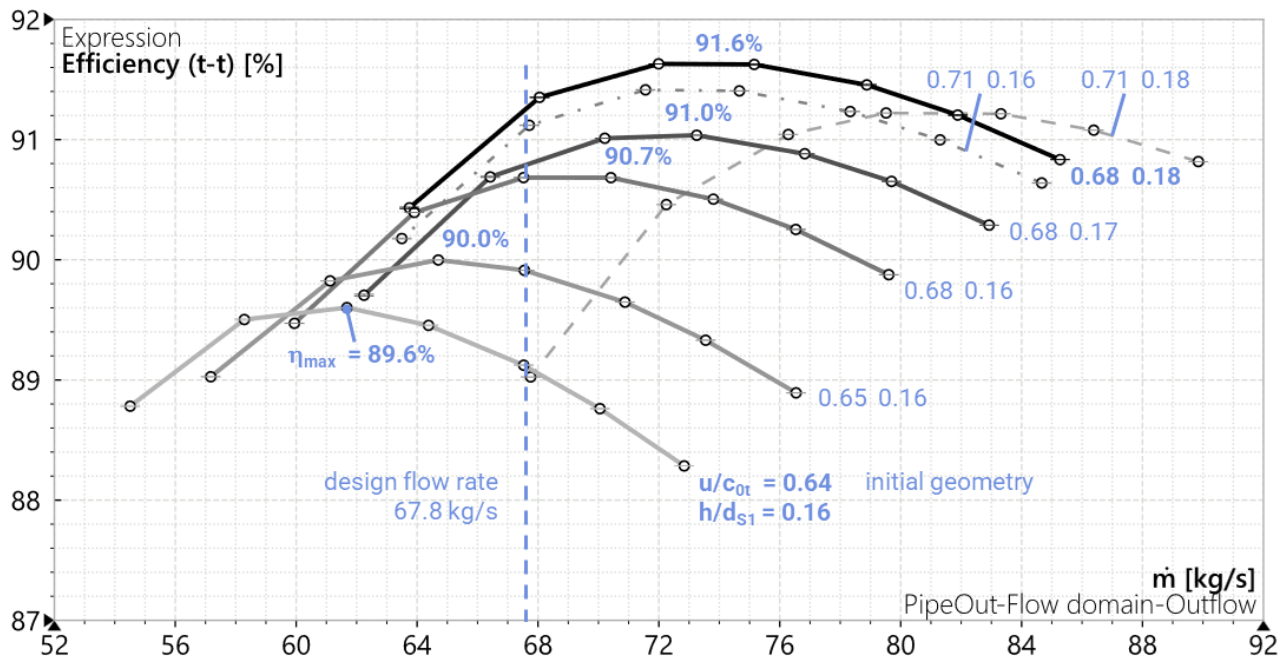


**Figure 9:** Total isentropic efficiency for the initial geometry and its variants

The variant with the highest peak efficiency is being further developed:  $u/c_{0t} = 0.68$ ,  $h/d_{s1} = 0.18$ . The desired shaft power is currently still achieved at a slightly higher mass flow rate of 73.5 kg/s (figure 10). The outlet flow from the rotor, which is already designed to be swirl-free, should remain largely unchanged, while the fluid redirection of the rotor inflow should be significantly increased by modifying the stator.

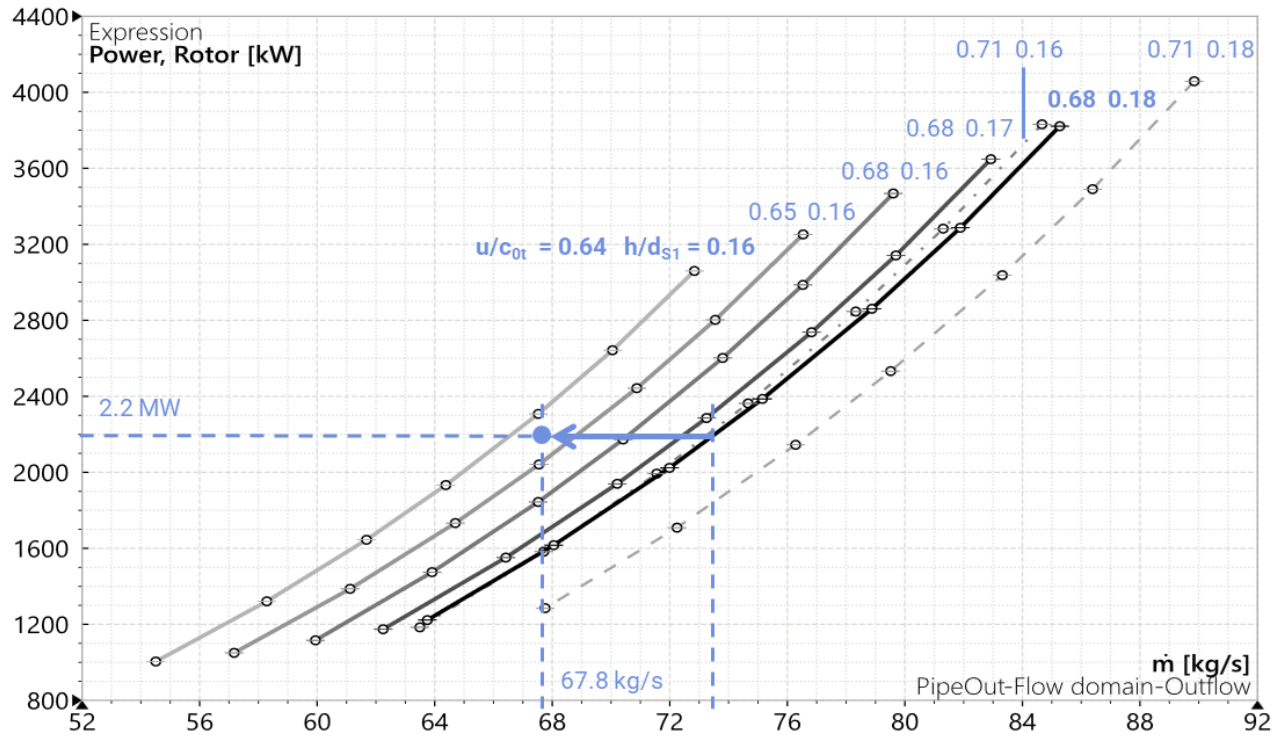


**Figure 10:** Shaft power curves: design point (blue dot) and necessary displacement (arrow)

The adjustment is performed systematically in CFturbo BLADERUNNER by cloning the initial geometry and then adjusting it iteratively (figures 11 and 12).

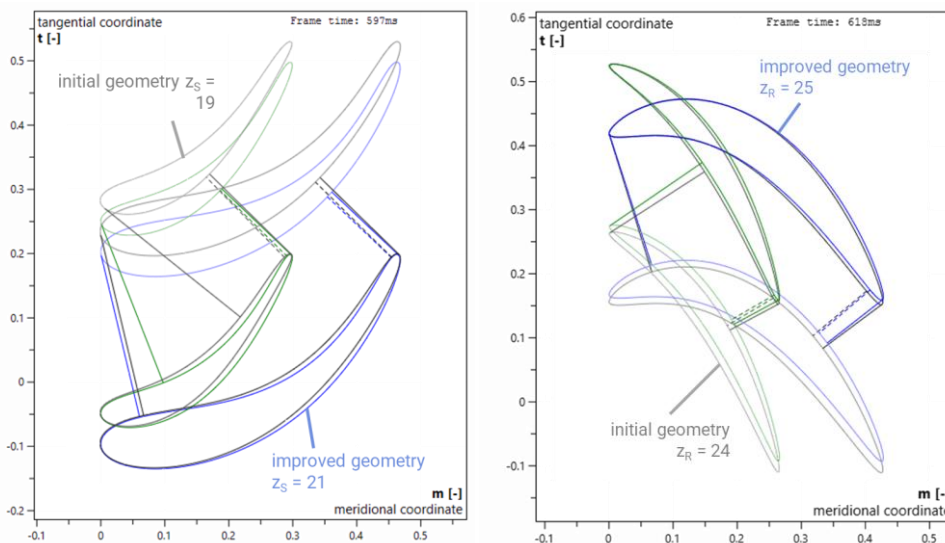


**Figure 11:** Changes to contours and number of blades on stator (left) and rotor (right): hub (blue), blade tip (green), original contours (gray)

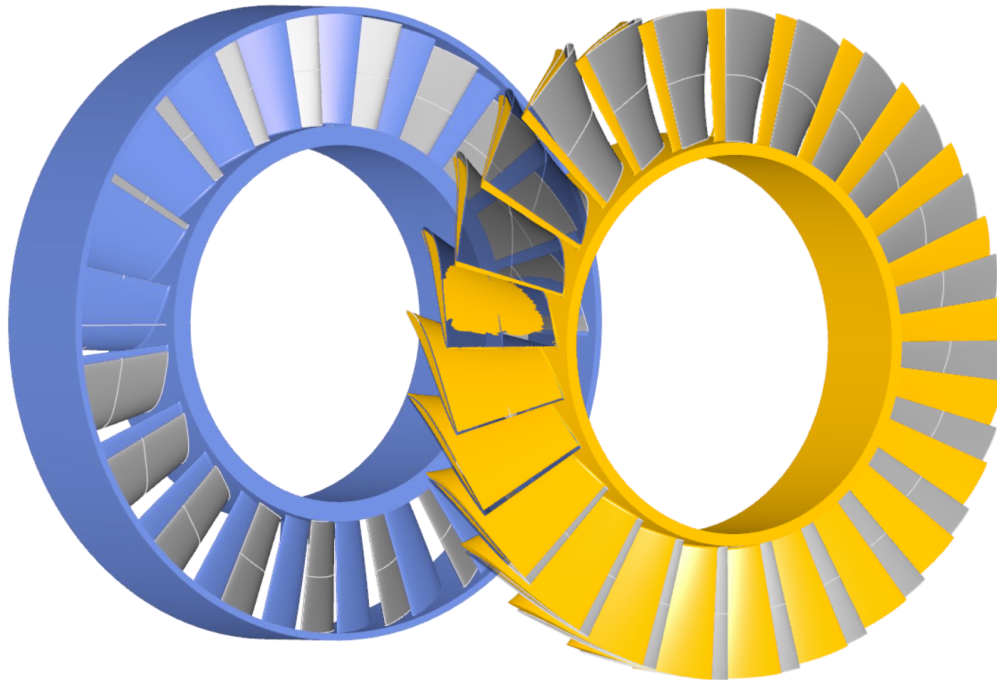


**Figure 12:** Overlay of the initial geometry (gray) with the final geometry of the stator (blue) and rotor (orange) in CFturbo

The steeper outlet angles and narrower flow channels result in a higher and more uniform flow redirection, so that both the desired shaft power is achieved and an even higher efficiency, the maximum of which now lies at the design point (figure 13). Reducing the gap at the rotor blade tips from 0.3 mm to 0.1 mm leads to a further increase in efficiency.

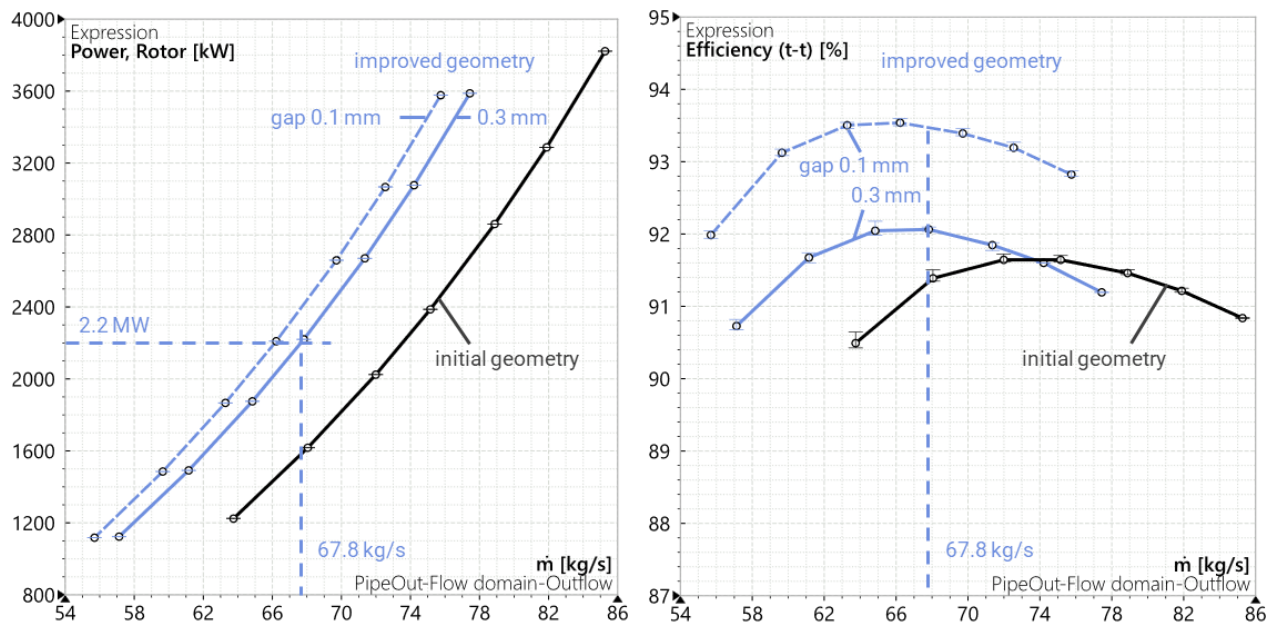


**Figure 13:** Comparison of shaft power (left) and isentropic efficiency (right)

Due to the radial balance in the rotor, the flow of the improved geometry runs on coaxial surfaces at the design point (figure 14, left) without any visible radial velocity component. Uniform expansion is achieved in the blade channels (figure 14, right). The flow in the rotor is blade-congruent.

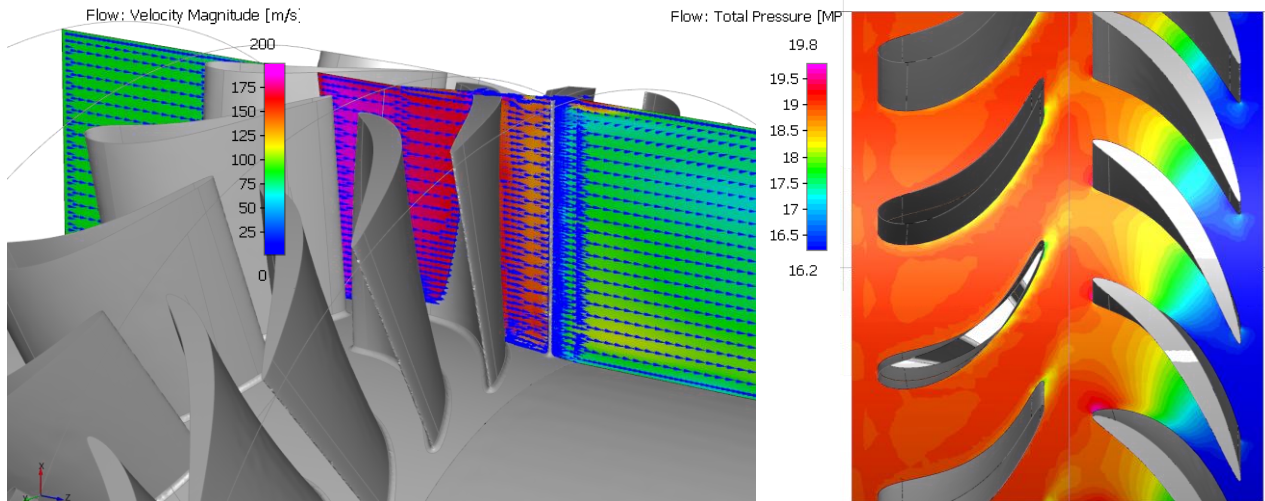


**Figure 14:** Radial section with projected flow vectors (left), total pressure pattern (right)

There is practically no residual swirl detectable downstream of the rotor, which indicates the best possible power extraction in the rotor (figure 15).

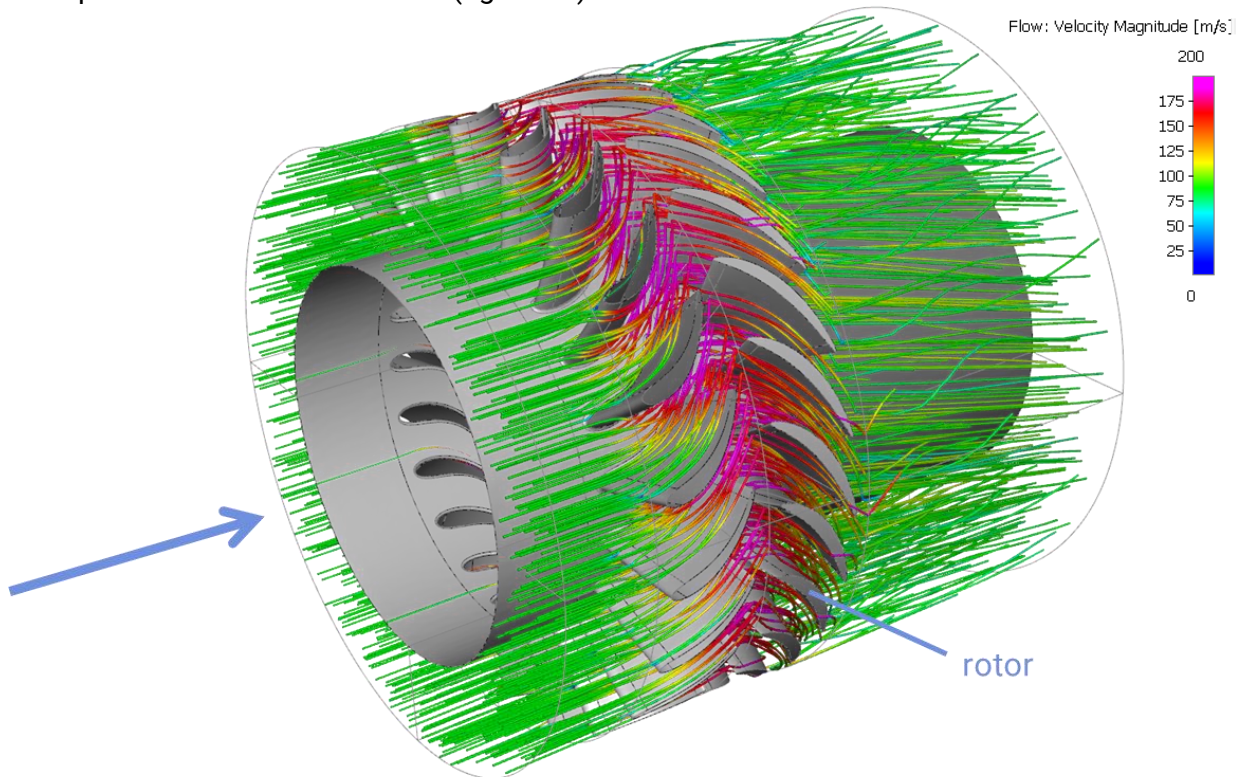


**Figure 15:** Streamlines with virtually no swirl downstream of the rotor

## CONCLUSION

The study describes all the essential design steps for a single-stage axial turbine of a rocket engine turbopump. Modern, user-friendly programs are used: CFturbo, CFturbo BLADERUNNER, and Simerics MP. It shows how a very good initial design with a few skillful modifications leads to the desired results. The required shaft power at the design point with high efficiency is achieved in just two design loops. In addition to expert knowledge, automated meshing and CFD simulation of the turbine characteristics are essential for the success of the process.

## LITERATURE

- [1] Vast Launcher on X, [x.com/launcher](https://x.com/launcher), 2025
- [2] ESA, [www.esa.int/Enabling\\_Support/Space\\_Transportation/Ariane/The\\_engines\\_of\\_Ariane\\_6](https://www.esa.int/Enabling_Support/Space_Transportation/Ariane/The_engines_of_Ariane_6), 2025
- [3] SpaceX on X, [x.com/SpaceX/status/1819772716339339664](https://x.com/SpaceX/status/1819772716339339664), 2025
- [4] Haeseler, D. et al., *Recent Developments for Future Launch Vehicle LOX/HC Rocket Engines*, AAAF-02-100, 6th International Symposium Propulsion for Space Transportation of the XXIst Century, 2002
- [5] Wikipedia, [en.wikipedia.org/wiki/SpaceX\\_Raptor](https://en.wikipedia.org/wiki/SpaceX_Raptor), 2025
- [6] CFturbo Inc., *CFturbo BLADERUNNER – Layout of an oxidizer centrifugal pump with consideration of cavitation*, study #3, 2025
- [7] Wikipedia, [en.wikipedia.org/wiki/Liquid\\_oxygen](https://en.wikipedia.org/wiki/Liquid_oxygen), 2025
- [8] Outcalt, Stephanie L., et al., *Thermophysical Properties Measurements of Rocket Propellants RP-1 and RP-2*, J. of Propulsion and Power, Vol. 25, No. 5, 2009
- [9] NASA CEA, [www.nasa.gov/glenn/research/chemical-equilibrium-with-applications/](https://www.nasa.gov/glenn/research/chemical-equilibrium-with-applications/)